International Journal of Pressure Vessels and Piping 193 (2021) 104436

Contents lists available at ScienceDirect

International Journal of Pressure Vessels and Piping

journal homepage: www.elsevier.com/locate/ijpvp

A methodology to prevent process piping failures during vapor cloud explosions

Ali Sari [a], Baris Sayin [b,*], Majid Pasbani Khiavi [c]

[a] Istanbul Technical University, Department of Civil Engineering, 34467, Istanbul, Turkey
[b] Istanbul University-Cerrahpasa, Department of Civil Engineering, 34320, Istanbul, Turkey
[c] University of Mohaghegh Ardabili, Faculty of Engineering, Ardabil, Iran

ARTICLE INFO

Keywords:
Blast failure
Process piping
Vapor cloud explosion
Finite element analysis
Pipe failure

ABSTRACT

The design and evaluation of offshore structures' piping systems subject to blast events are of significance and require advanced analysis approaches. They are important because during an explosion rupture of a piping and vessel system leads to the leakage or release of hydrocarbons which will likely cause another explosion. Advanced nonlinear analysis in time domain is required in order to agreeably determine the dynamic behavior of the piping and vessels against blast loadings. A linear approach, for example using Caesar II software package, often gives very conservative results. This conservative design approach results in pipes and vessels with high wall thickness. Such pipes and vessels bring more weight to offshore facilities and are not desirable, especially for floating structures. In other words, advanced non-linear time domain analysis is required if weight reduction is a must. This analysis type, broadly, should consider; i. Drag load and blast overpressure, ii. Nonlinear material features for instance thermal and strain-rate dependence, iii. Effects of nonstructural masses and adjacent piping systems; iv. Pipe supports, v. Failure of flanges and piping detail, vi. Effects of operating temperature on material characteristics, vii. Blast direction/Ignition location/Attenuation sensitivity; viii. Shielding effect, i.e. pipes behind large objects such as vessels, and ix. Effects of pipe insulation, e.g. raised pipe diameters. The study, firstly, examines the approach/techniques to describe for such effects with finite element analysis. This paper then uses case studies to demonstrate the methodology that includes advanced simulation techniques for pipe blast behavior. The case studies include a piping system that is simulated from overall to detail modeling. Simulations are carried out using the general-purpose, FEA package, ABAQUS. The goal of the paper is to discuss the challenges and propose the methodology for realistic simulation of response of a piping system in a blast event. The paper is expected to serve as a complimentary example to recommended practice (FABIG Technical Notes and API 2FB 2006).

1. Introduction

Assessment of offshore structures' piping systems against blast is needed because failure or rupture of a piping/vessel system can lead to subsequent explosion events. Nonlinearities should be considered because linear response approach often results in very conservative design which might cause difficulties to reduce weight of the structure.

Recommended procedure for the design of piping against explosions was documented in FABIG Technical Note [1] and API 2006 [2]. The methodology of performance based design of blast resistant offshore piping has also been described in recent studies including a report produced for HSE by SCI in 2005 [3] and a paper by Yasseri and Ocraft [4] in 2010. However, up to date, there is little discussion on an advanced approach that includes all aspects of a piping blast analysis. This paper attempts to give an overview of considerations that should be included in the analysis. The first part of the paper discusses these considerations. The second part serves as demonstration to the methodology by cases studies. This part of the paper includes three ABAQUS [5] simulations involving a Vapor Recovery Unit (VRU) piping system modeled at different detail levels. In the first simulation, the VRU system was modeled using beam elements; this simulation is referred to as Beam Model. Using shell element, the second simulation looked into more details of response of a vessel and pipes connected to it; this simulation is referred to as Shell Model. The third simulation, referred to as Solid

* Corresponding author.
E-mail address: barsayin@iuc.edu.tr (B. Sayin).

https://doi.org/10.1016/j.ijpvp.2021.104436
Received 15 March 2021; Received in revised form 26 April 2021; Accepted 6 May 2021
Available online 15 June 2021
0308-0161/© 2021 Elsevier Ltd. All rights reserved.

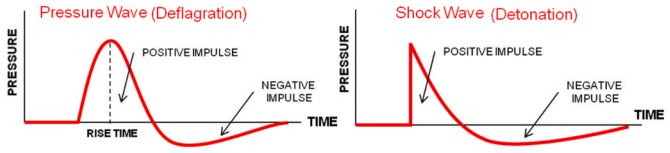

Fig. 1. Typical overpressure time history for two types of explosions.

Model, involved sub-modeling of a pipe flange using solid elements. In the Solid Model, the flange's boundary conditions were fed from the Beam Model, in which the flange was modeled as shell elements. More details of modeling for each case are followed.

2. Methodology

Piping blast analysis in general should take into account the following considerations as i. The effects of drag load vs blast overpressure, ii. Nonlinear material model, iii. Effects of non-structural masses and adjacent piping systems, iv. Pipe supports, v. Flange failure, vi. Effects of operating temperature on material properties, vii. Blast direction/Ignition location sensitivity, viii. Effects of shielding, ix. Effects of pipe insulation.

Sketch	Shape	C_d
Flow	Circular cylinder (long rod), side on	1.20
	Sphere	0.47
Flow	Rod, end-on	0.82
or Flow	Disc, face-on	1.17
Flow	Cube, face-on	1.05
Flow	Cube, edge-on	0.80
Flow	Long rectangular member, face-on	2.05
Flow	Long rectangular member, edge-on	1.55
Flow	Narrow strip, face-on	1.98

Fig. 2. Drag coefficients, C_d, for various shapes [6].

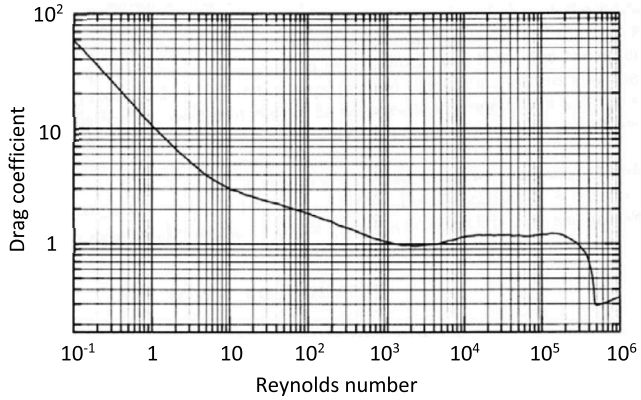

Fig. 3. Drag coefficient of a cylinder as a function of Reynolds number [7].

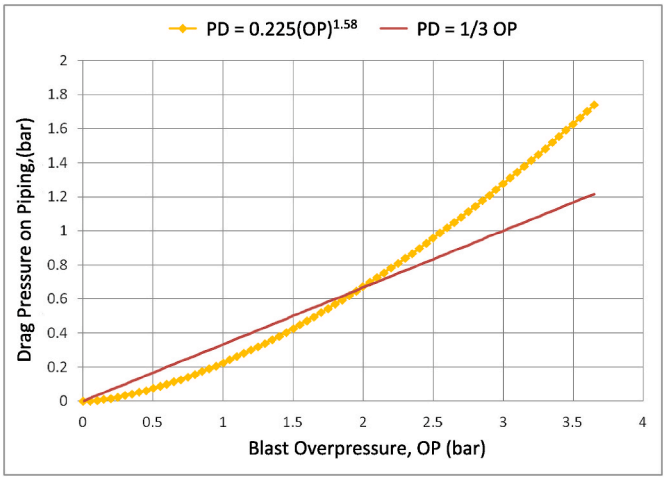

Fig. 4. Blast drag pressure versus overpressure for a typical offshore module [4].

2.1. Blast drag loading versus blast overpressure effects

Two class of loading that must be deemed in the piping blast analysis are overpressure and drag. Similar to building structures, big pipes and vessels respond to both overpressure and drag loadings; while small pipes respond mostly to drag pressure.

The distribution of pressure around a cylinder results in a time varying force in the stream-wise and the crosswise direction. The hydrodynamic force is calculated by integrating the normal- and shear-stresses over the surface of the obstacle. The following formula shows a phenomenological splitting of the hydrodynamic force [3]:

$$F_h = \frac{1}{2} C_d A|U(t)|U(t) + (\rho V + m)\frac{\partial}{\partial t}(U) + \frac{\partial \rho}{\partial t} VU(t) + F_{DP(M)} + F_{HE} \quad (1)$$

where U is the flow velocity and V is the volume of the fluid. The first term is the quasi-static form drag force depending on obstacle shape, surface roughness, fluid density and Reynolds number. The second term is the inertia force which is proportional to the acceleration. The third term is a combustion contribution originating from the modification of mass per unit volume in a generalized form of Newton's law. The fourth term is the differential pressure, which is a function of the mach number (U/c), where c is the velocity of sound. The last term is the hydro-elastic component which is related to the effect of structural response of body and the fluid around it.

2.1.1. Blast overpressure

Overpressure is the pressure resulting from a shock wave over and above normal atmospheric pressure. Blast overpressure results from explosions which can be classified into two types: detonation and deflagration. *Detonation*, e.g. generated with TNT, occurs when the combustion is lead by shock heating and pressurization of the unburned fuel to the point of auto-ignition. *Deflagration,* e.g. vapor cloud explosions, is mostly a subsonic combustion event where the hot burning material preheats the subsequent layer of cold unburned gas or dust and ignites it. Fig. 1 shows typical overpressure time history for two types of explosions. As illustrated in Fig. 1, the rise time for detonation type is almost instant while that of deflagration can be between 20% and 75% of the positive impulse duration. Deflagration times of development are on the order of few milliseconds while that of detonation is a lot shorter, on the order of millionths of a second.

2.1.2. Blast drag loading

The drag force, a combination of the skin friction (tangential stresses) and the form drag (normal stresses), is mostly stated as follows:

$$F_D = \frac{1}{2}\rho A C_d |v| v \quad (2)$$

where ρ is the fluid density, A is the maximum cross sectional area of the object in a plane normal to v , C_d is the drag coefficient, and v is the large scale fluid velocity ignoring spatial fluctuations in the vicinity of the object.

To allow the drag loading to be applied in the finite element models, blast pressure must be converted to an equivalent distributed load, i.e. drag force. The drag force is rewritten using the formula below:

$$F_D = C_d P_d OD \quad (3)$$

where.

F_D = Drag force
C_d = Drag coefficient
P_d = Drag pressure [psi]
OD = Outer diameter of the pipe

In summary, with the drag pressure known, a line load was computed by multiplying the drag pressure by outer diameter of the pipe/tube being loaded. The force is then multiplied by a drag coefficient, C_d, to get the drag line load. The drag coefficient, C_d, rely on the shape of the obstacle and on the Reynolds number of the flow. The nature of C_d has been examined extensively for various standard shaped objects in steady flow. Fig. 2 presents the drag coefficient for different shapes which suggests a value of 1.2 for pipes. Dependence of C_d on the Reynolds number is summarized in Fig. 3, for flow transverse to a cylinder.

In Equation (3), the drag pressure may be computed as approximately 1/5 to 1/2 of the blast overpressure (OP). Recall that the dynamic pressure is specified as 1/2 the fluid density times the square of the fluid velocity.

$$q = \frac{1}{2}\rho v^2 \quad (4)$$

The Rankine-Hugoniot relation [8] defines the magnitude of the dynamic pressure as a function of the overpressure, OP, and the ambient pressure, P_0.

$$q = \frac{5}{2}\frac{OP^2}{(7P_0 + OP)} \quad (5)$$

Fig. 4 shows a CFD-based empirical relation and the approximated one between blast drag pressure on piping and overpressure calculated using CFD analysis for a typical offshore module [4]. Using 1/3 coefficient gives conservative drag pressure up to an overpressure of approximately 2 bars (1 bar is 14.5 psi). The CFD empirical relation is as

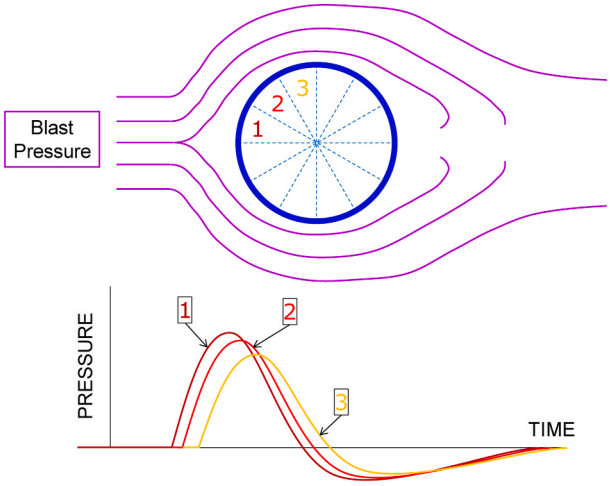

Fig. 5. Pressure time delay and attenuation with large pipes.

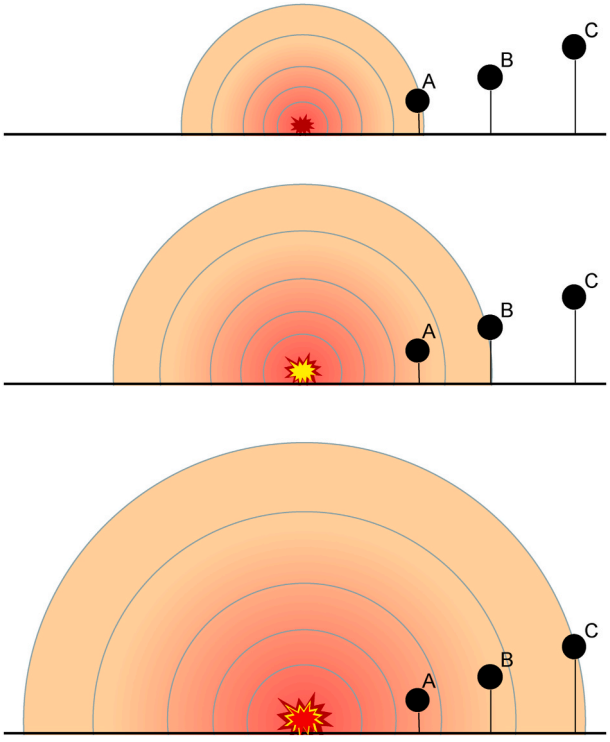

Fig. 6. Blast wave propagation.

follows

$$P_D = 0.228(OP)^{1.58} \quad (6)$$

Ideally, a CFD (Computational Fluid Dynamics) analysis should be performed first to computer the blast loads on a pipe system. Results of the CFD analysis is then fed into a FEA (finite element analysis) which predicts structural response of the pipe system through a nonlinear transient dynamics solver. However, the main problem with CFD approach is that in order to capture drag load around a pipe section properly, fine mesh is often required; hence expensive in computational cost. With small pipes, response to explosion wind (drag pressure) is dominant to response to overpressure. In other words, overpressure (direct shock loading) is small compared to drag pressure (explosion wind). This is primarily due to the speed with which shock fronts can pass piping systems, enabling rapid equalization of upstream and downstream pressures [1]. However, this might not be true with pipes or vessels with one-foot diameter or larger [3]. With these large pipes, pressure does not wrap around pipe section quick enough to establish equalization. As a result, upstream and downstream pressures are not in balance and there are time delay and attenuation in terms of pressure as shown in Fig. 5. In other words, effects of overpressure might not be negligible and should be considered in analysis.

The phenomena of time delay and attenuation with large pipes is

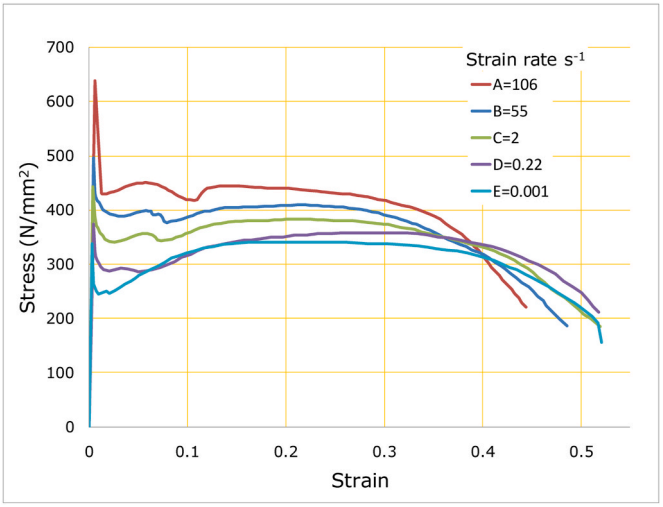

Fig. 7. Effect of strain rates on behavior of mild steel [9].

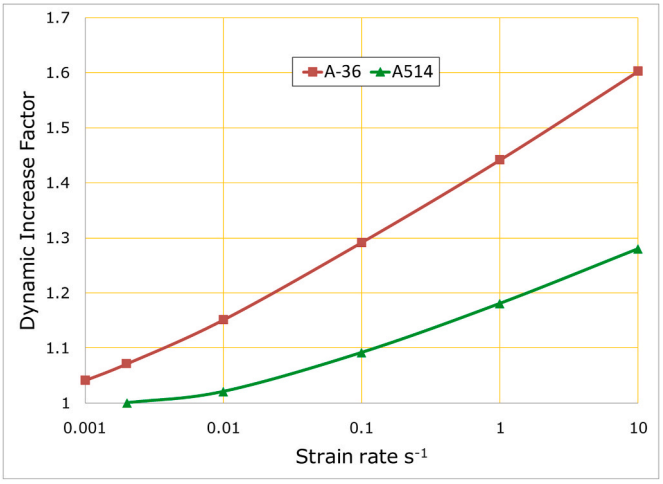

Fig. 8. Dynamic increase factor for yield strength of mild and high strength steel versus strain rate [10].

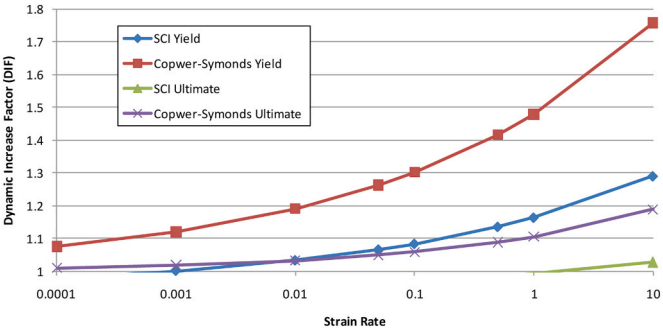

Fig. 9. Dynamic increase factor of 50 ksi mild steel versus strain rate.

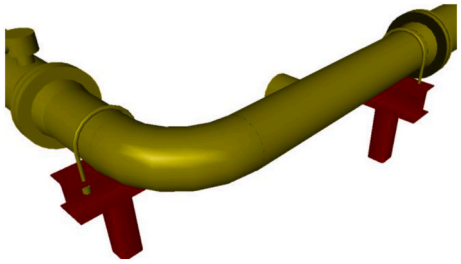

Fig. 10. Example of pipe supports and U-bolts.

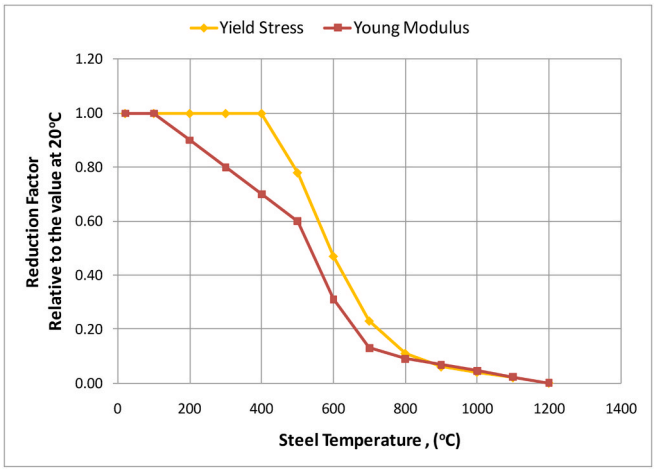

Fig. 11. Reduction factors for stress vs strain relationship of carbon steel at elevated temperatures [13].

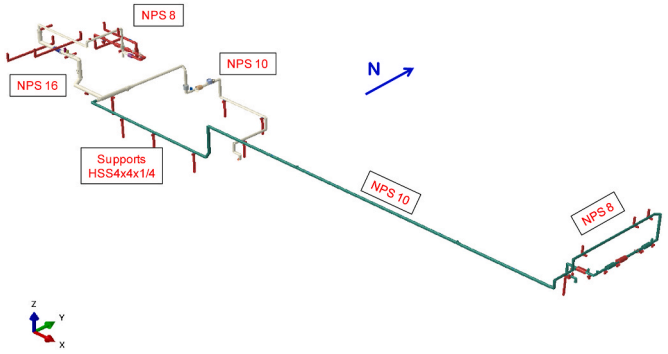

Fig. 12. FE beam model showing pipes and supports.

Table 1
Pipe size and material properties.

NPS	Schedule	Outside diameter (inches)	Thickness (inches)	Material
8	10 S	8.625	0.148	BE Smls ASTM A790 UNS-S31803
10	10 S	10.75	0.165	BE Smls ASTM A790 UNS-S31803
16	10 S	16	0.188	BE Smls ASTM A790 UNS-S32750

similar to the way blast wave propagates in space. Fig. 6 illustrates how blast wave travels toward objects A, B, and C. Given the ignition location, each object experiences blast pressure differently. Being closest to the ignition location, object A experiences blast loads first. Blast wave

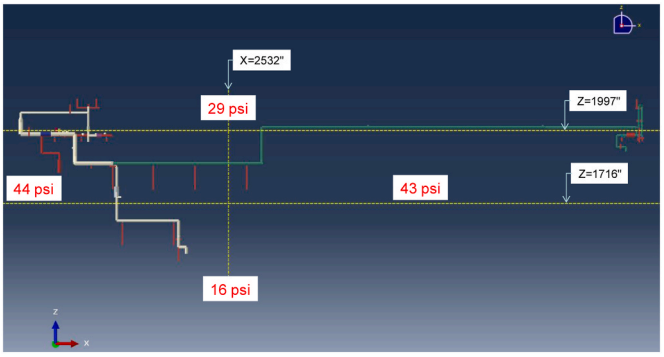

Fig. 13. FE beam model showing blast load criteria.

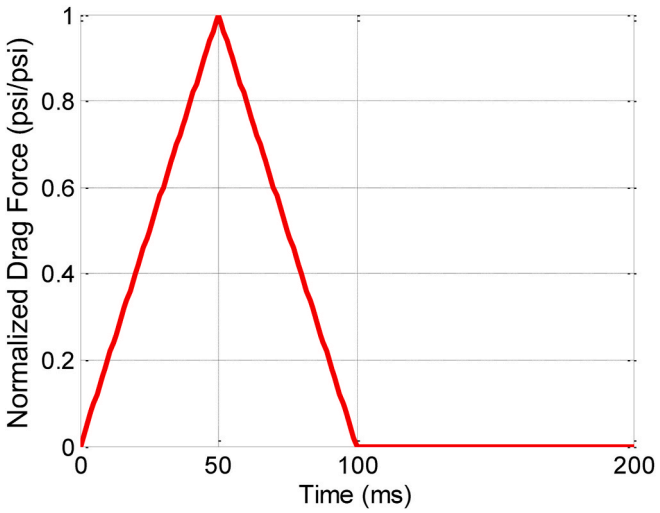

Fig. 14. Normalized drag force time history.

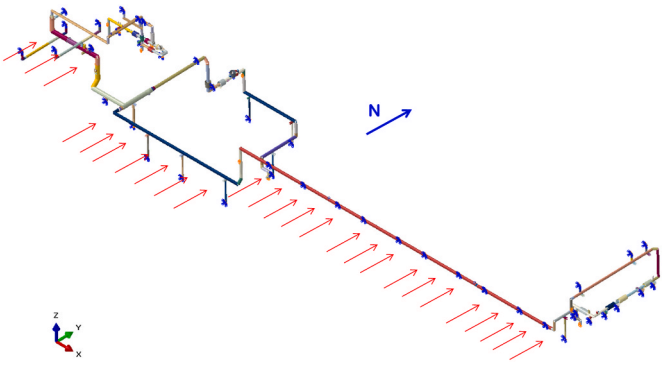

Fig. 15. Boundary conditions and loading in +Y direction.

comes to object C last with less pressure compared to blast wave at A and B. Blast drag pressure time history at A, B, and C will look similar to those shown in Fig. 5 but at a larger magnitude of difference. These effects should also be considered in a piping blast analysis.

2.2. Nonlinear material model

Excessive deformation and failure of pipes are expected throughout a blast event. Therewith, nonlinear geometry should be considered. Note that Abaqus/Explicit [5] uses true stress/strain data for material plasticity definition and material plasticity/failure must be modeled to reflect these nonlinear effects. As blast loading happens in very short

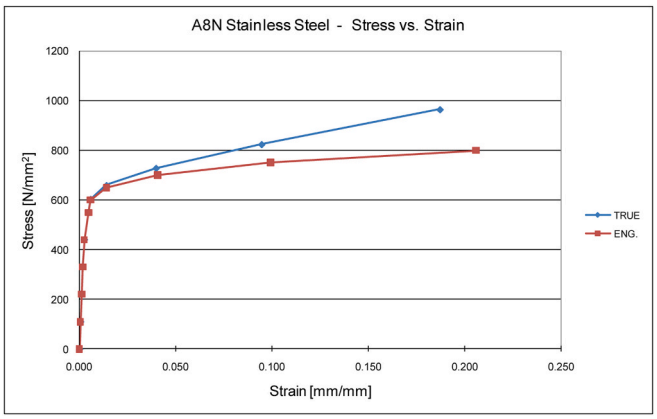

Fig. 16. Stress-strain relationship for stainless steel material.

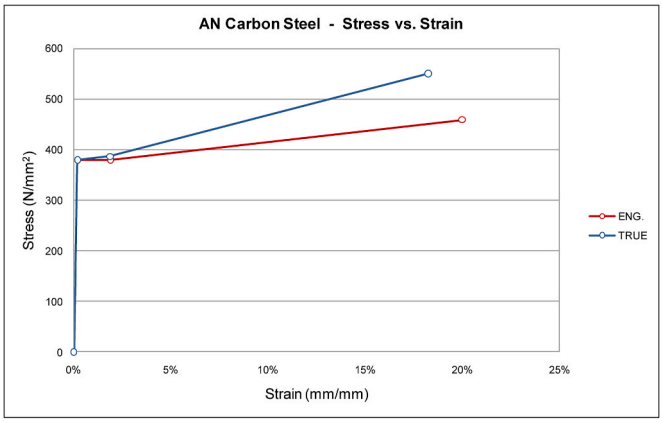

Fig. 17. Stress strain relationship for carbon steel material (AN).

duration of time, rate-dependent plasticity should be considered. Fig. 7 offers stress-strain relationships up to fracture for low-carbon mild steel at various strain rates [9]. Yielding stress is, as well, sensitive to strain rates, particularly for high strength steels. Increase in yield strength depending on strain rate effects is characterized by a dynamic increase factor. In Fig. 8, the dynamic increase factor for yield strength versus strain rate is schemed for a mild steel (ASTM A36 steel with static yield stress of 250 MPa) and for a high strength, quenched and tempered steel (ASTM A514 steel with yield stress about 760 MPa) [10].

Cowper and Symonds [11] proposed a relationship which can be used to compute the enhancement of stresses in consequence of strain rate effects. The relationship is stated as follows:

$$\frac{\sigma_D}{\sigma_S} = 1 + \left(\frac{\dot{\varepsilon}}{D}\right)^{\frac{1}{q}} \tag{7}$$

where.

σ_D = Dynamic stress at a particular strain rate
σ_S = Static stress
$\dot{\varepsilon}$ = Uniaxial plastic strain rate
D and q = Constants associated with steel

Values of D and q are strain-dependent. For example, $D = 40.4\ s^{-1}$ and q = 5 could be used to describe the behavior up to 4% strain of mild steel. Despite its popular use, recent tests [12] indicate that Cowper and Symonds model might be un-conservative as shown in Fig. 9. The SCI relation, illustrated in Fig. 9, recommended for mild steel is as follows;

$$\sigma_{Dy} = \sigma_t - 25 + 210\left(\frac{\dot{\varepsilon}}{D}\right)^{\frac{1}{q}} \quad \text{(MPa)} \tag{8}$$

where.

σ_{Dy} = Dynamic yield stress at a particular strain rate
σ_t = Specified minimum yield stress

2.3. Effects of non-structural masses and adjacent piping systems

It is common that pipe systems are designed to run parallel to each other sharing the same support or run along a wall. A piping blast analysis should take into account the possibility that a pipe can impact other pipes or walls because of excessive deformation of pipes that can occur. Flanges, valves, and fittings should be taken into account as nonstructural masses. Non-structural masses can also come from adjacent piping system sharing the same supports. In general, these masses change the dynamic response of the piping system in a conservative way, i.e., more mass, less displacement. However, for a particular location, the above statement is not always valid. It is desirable to include these effects in analysis.

2.4. Pipe supports

Interaction among pipe and support and U-bolts should be considered. Assumptions on supports in piping blast analysis can significantly

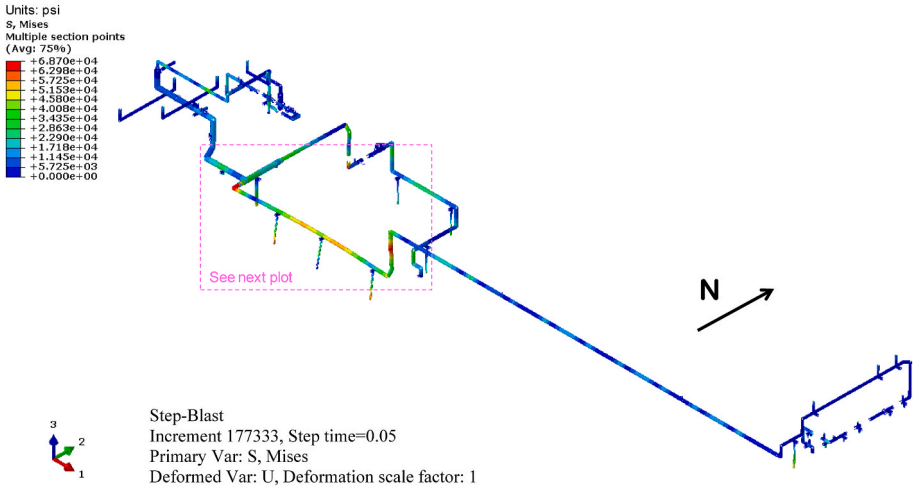

Fig. 18. Effective stress contour at time = 50 ms

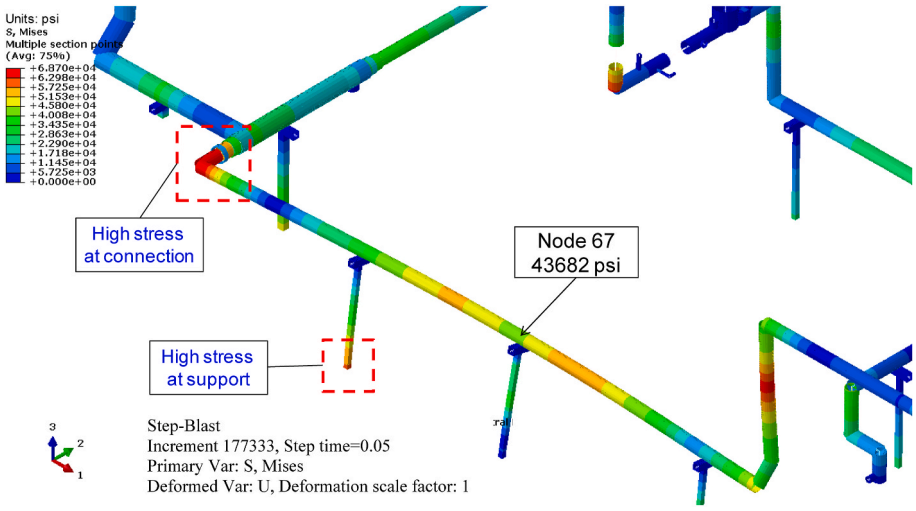

Fig. 19. High stress at pipe connections and supports at time = 50 ms

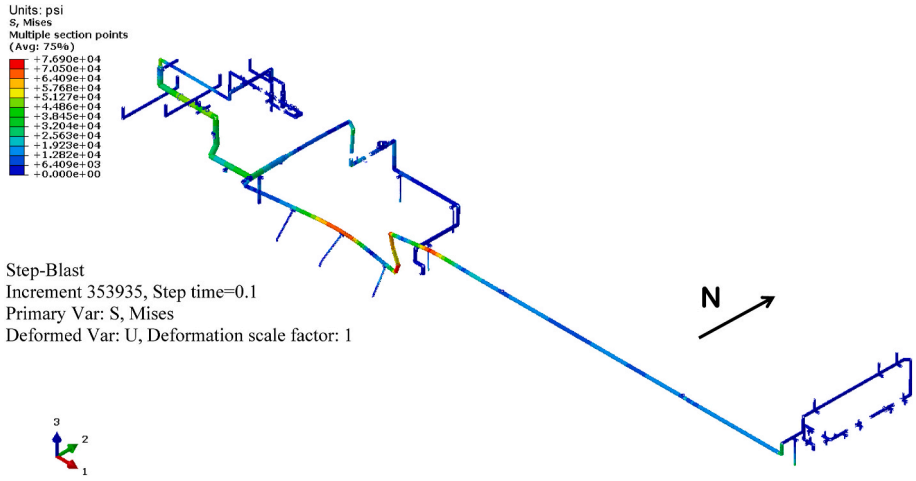

Fig. 20. Effective stress contour at time = 100 ms

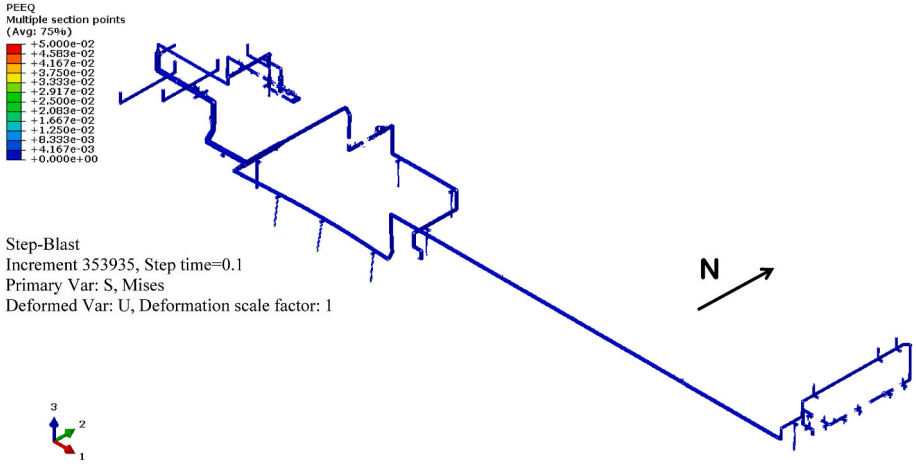

Fig. 21. Plastic strain contour at time = 50 ms

affect analysis results. Pipe supports can fail during a blast. Assuming pipes are fixed or pinned at supports then using corresponding reactions to analyze supports can be fallacious. In other words, in blast analysis, care should be taken when modeling pipe supports. They should be modeled explicitly. Fig. 10 shows an example of pipe supports and U-bolts from a 3D model view in which pipe supports and U-bolts are modeled as shell and beam element, respectively. If pipe supports are not explicitly included in analysis, i.e., they are modeled as an

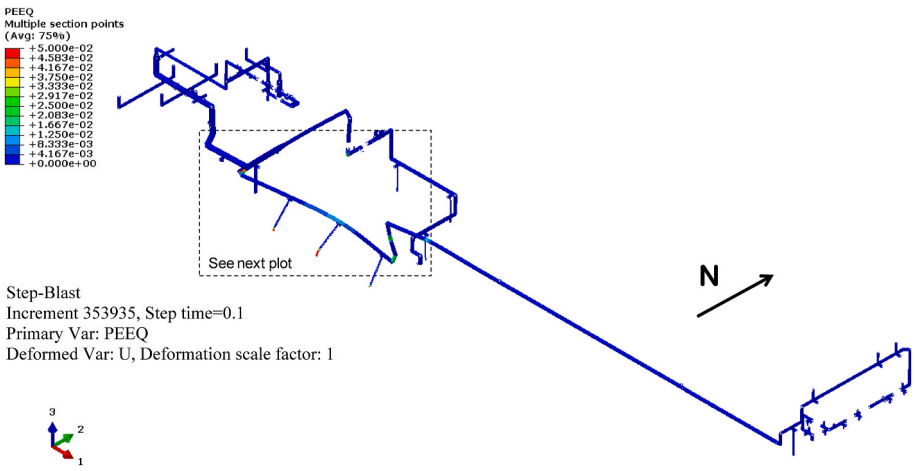

Fig. 22. Plastic strain contour at time = 100 ms

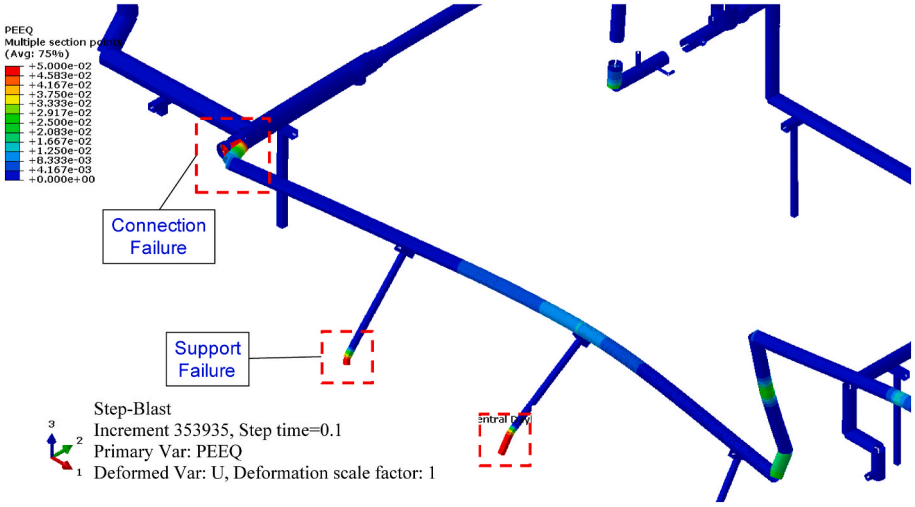

Fig. 23. Plastic strain of pipe connection and supports at time = 100 ms

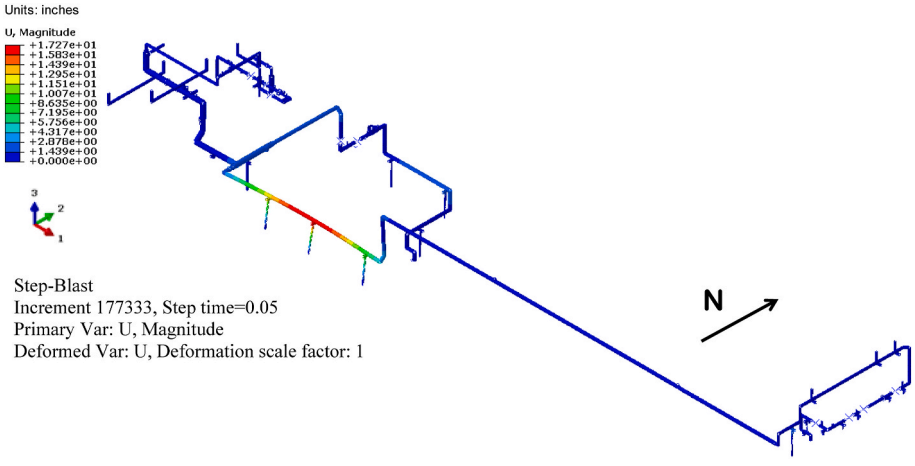

Fig. 24. Deflection contour at time = 50 ms

"absolute" boundary condition such as pinned, fixed conditions, i.e. pipe support detail cannot fail, the displacements at these support locations remain zero throughout the analysis which effectively change the dynamic response of the entire system. In general, this results in less piping displacement at mid-span locations but higher piping stresses at support locations. In other words, stress results are unrealistically conservative while displacement results are un-conservative.

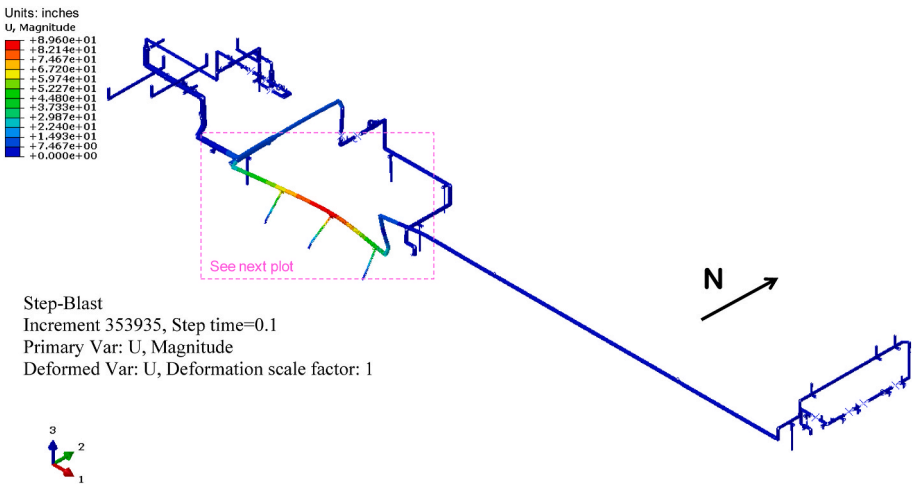

Fig. 25. Deflection contour at time = 100 ms

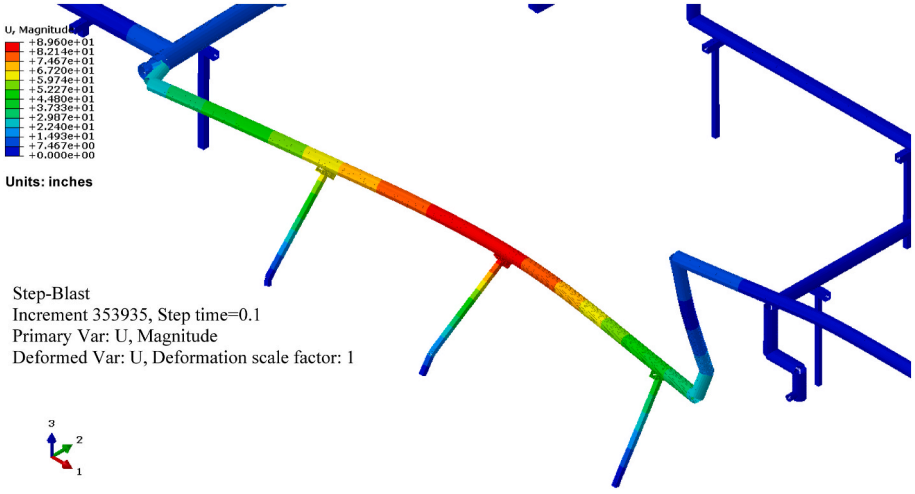

Fig. 26. Large deflection at end of blast loading (time = 100 ms).

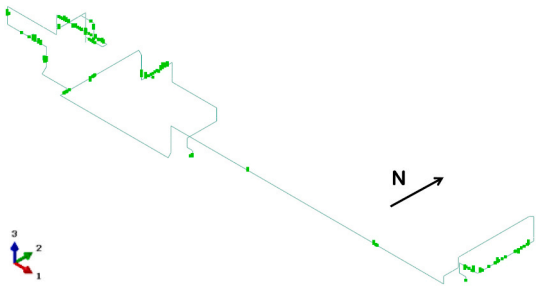

Fig. 27. Non-structural mass assignments.

2.5. Flange failure

In a blast event, pipes might deform excessively without rupture and without release. However, details such as flanges and fittings can fail because they may have less strength in bending than the pipe in which they are located. Such failure can give rise to an escalation of an initial explosion event to the failure of larger vessels and/or pipes. This is discussed later in some more details in the Solid Model.

2.6. Effects of operating temperature on material properties

Material properties in general are temperature dependent. Although for pipe systems the effect of operating temperature is limited, steel Young modulus is reduced when the operating temperature is over ~100° Celcius. This stiffness reduction should be included in a piping blast analysis. Fig. 11 shows an example of carbon steel properties as a function of temperature (known as degradation curves). It is indicated from Fig. 11 that Young modulus is more sensitive to temperature than yielding stress.

2.7. Blast direction/ignition location sensitivity

Blast loading is directional. However, it is common conservative practice that blast loading is assumed principal directions with respect to the piping systems provided information on blast loading is not known [1]. However, a sensitivity study on blast direction/ignition location should be conducted to check if other directions can be more critical to the pipe system response.

If the pipe system is long, the differential blast pressure along piping length due to the attenuation of the blast overpressure or drag along with distance and the time differences of the peak pressures should also be considered.

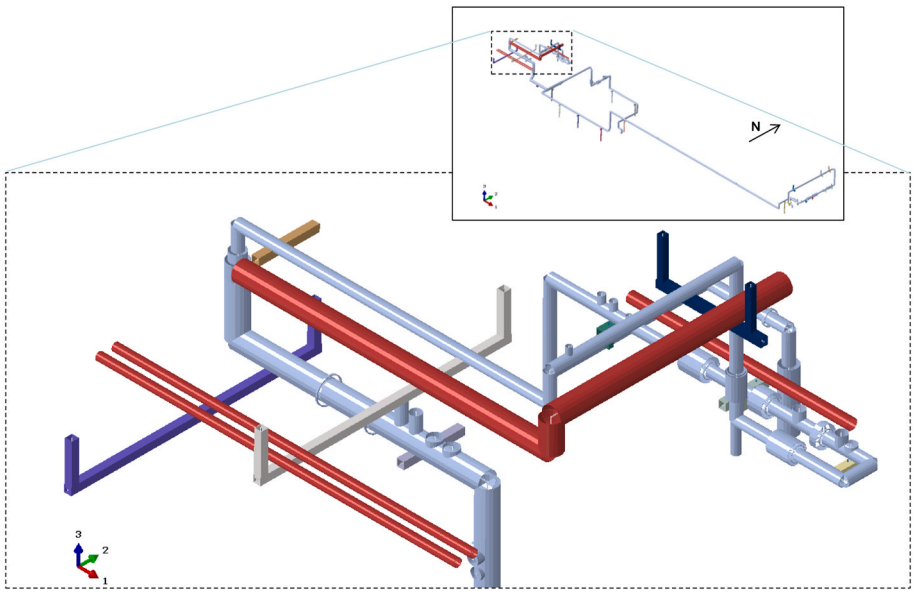

Fig. 28. Other piping systems (shown in *red*) sharing same supports with VRU. (For interpretation of the references to colour in this figure legend, the reader is referred to the Web version of this article.)

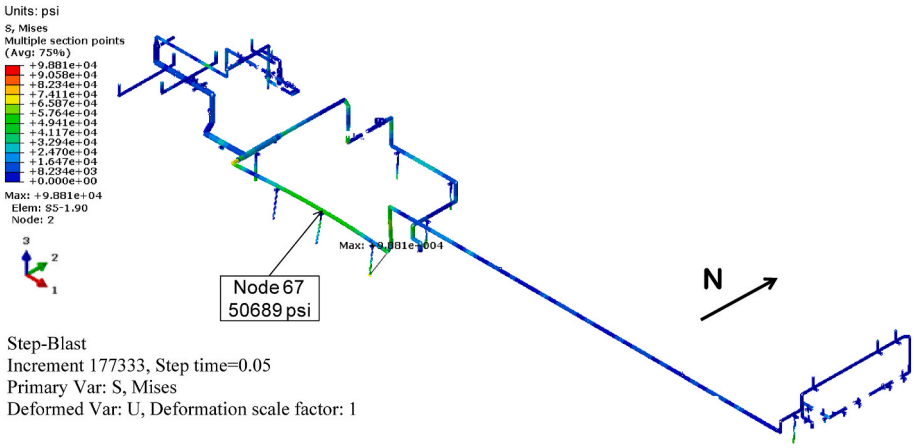

Fig. 29. Effective stress contour at time = 50 ms (compared with Fig. 18 and 19.).

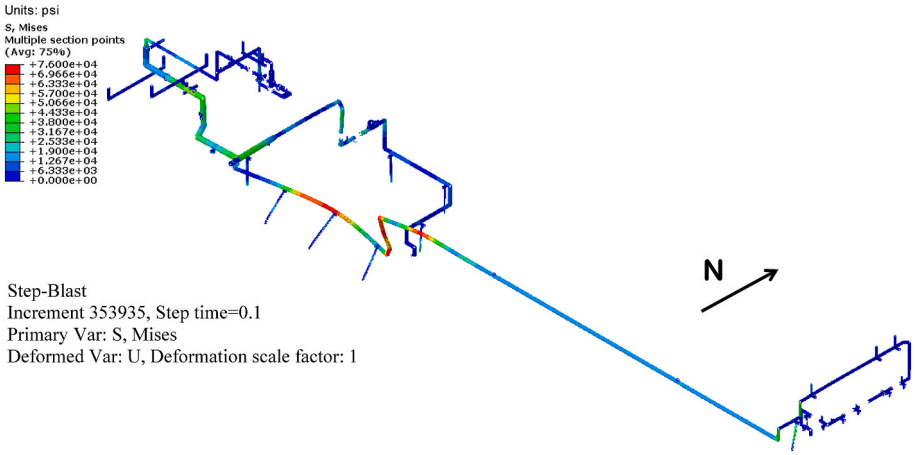

Fig. 30. Effective stress contour at time = 100 ms (compared with Fig. 20.).

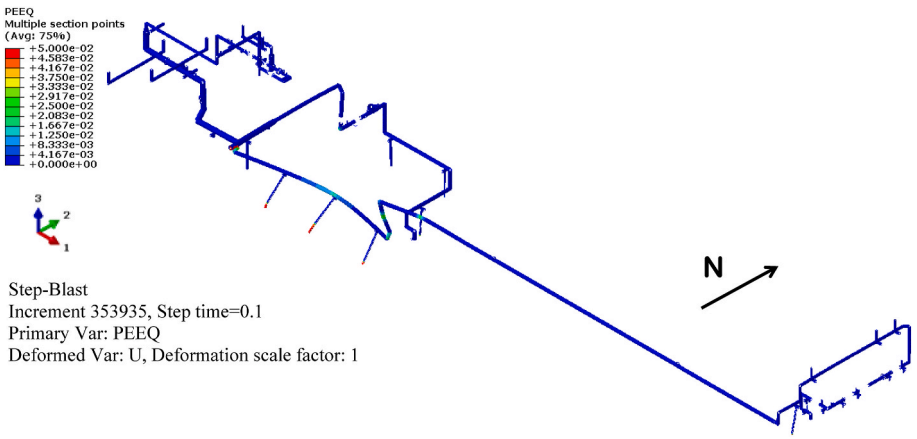

Fig. 31. Plastic strain contour at time = 100 ms (compared with Fig. 22.).

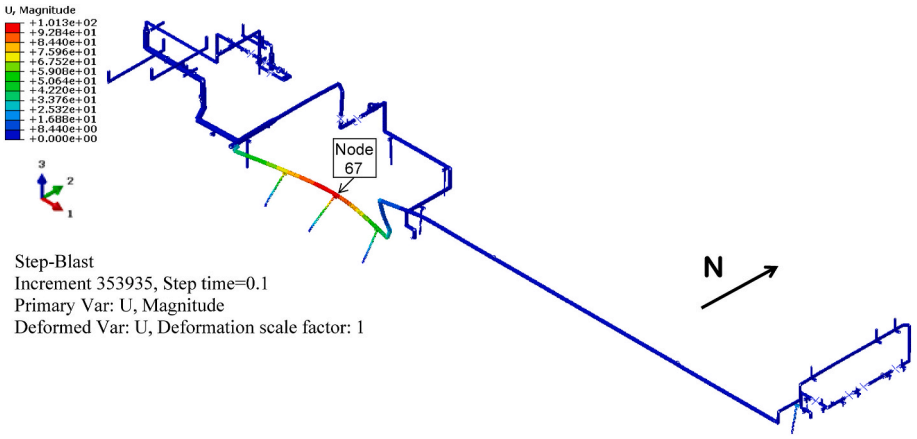

Fig. 32. Deflection contour at time = 100 ms (compared with Fig. 25.).

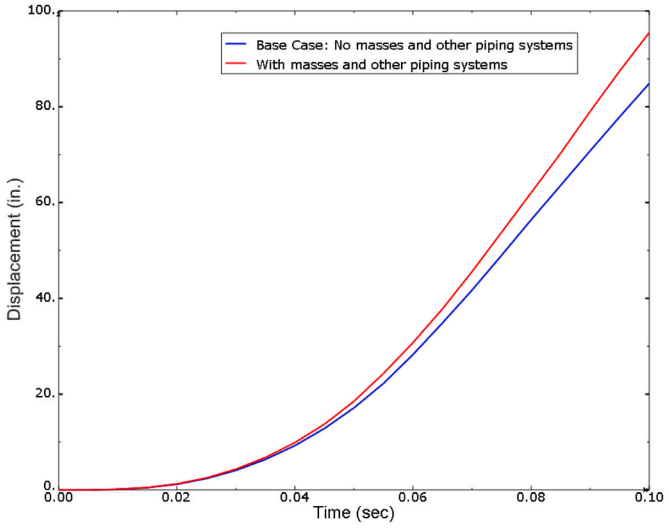

Fig. 33. Displacement time history of node 67 (see Fig. 32.).

2.8. Shielding effects

In an explosion, a certain amount of blast pressure reduction may be gained by having any large and substantial object between the object of interest and the ignition location. For example, in a blast event, a vessel between a pipe and the explosion center will shield the pipe from the explosion, partially reducing the blast pressure on the pipe. This shielding effect might be included in a piping blast analysis.

2.9. Pipe insulation

Pipe insulation help protect pipes from freezing and condensation when operating at low temperatures. Very hot pipe systems should also be insulated to avoid potential human injuries. In terms of loading, insulation leads to larger pipe outer diameter, which technically attracts more drag loads in a blast event. As shown in Equation (3), the blast drag force is linearly proportional to the outer diameter of the pipe. In general, pipe insulation thickness is a function of pipe temperature and pressure. Drag pressure should be calculated based on effective outer diameter which takes into account pipe coatings.

3. Case studies

All analysis models taken into account in case studies are for pipe systems of existing facilities.

3.1. Analysis assumptions

The following assumptions were made in the subsequent case studies:

Blast loading.

- Drag pressure was assumed to be 1/3 of overpressure;

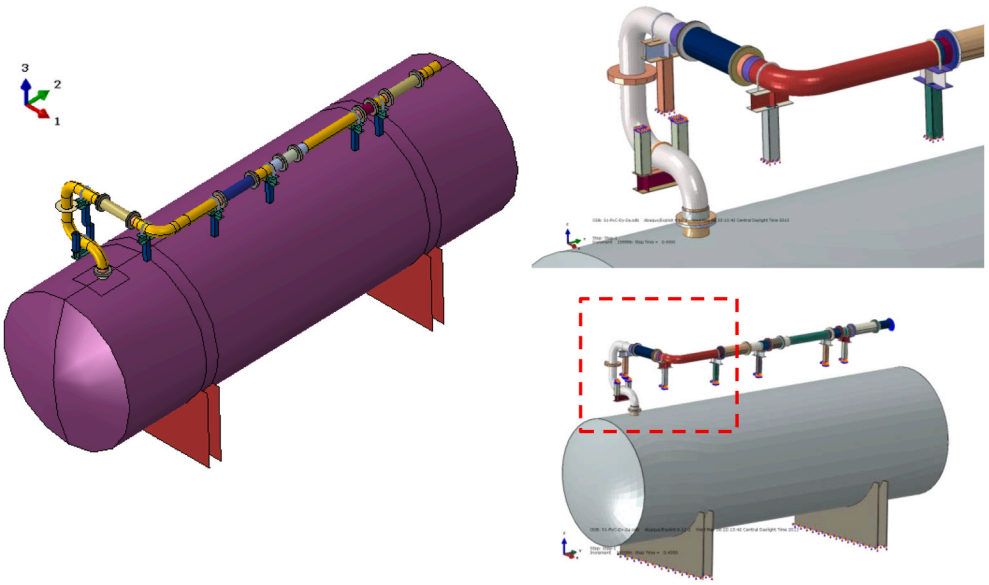

Fig. 34. VRU system FE shell model.

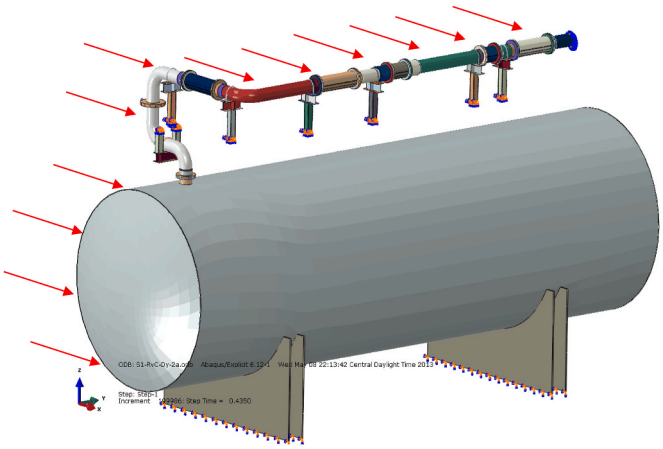

Fig. 35. Loading in +X direction.

- The drag coefficient was assumed to be 1.2;
- Blast loading is applied in principal directions, +/-X, +/-Y and ± Z, with respect to the piping systems; this is typical provided information on blast loading is not known [1].

Boundary conditions.

- In beam models, U-bolts were modeled as springs; supports were modeled explicitly as beam elements;
- Pinned connection was assumed at pipe-vessel connections.
- Pipes were transversely restrained at deck penetration.
- Pipe support components were assumed to be fixed.

Material.

- 10% reduction in Young modulus due to operating temperature

Failure criteria.

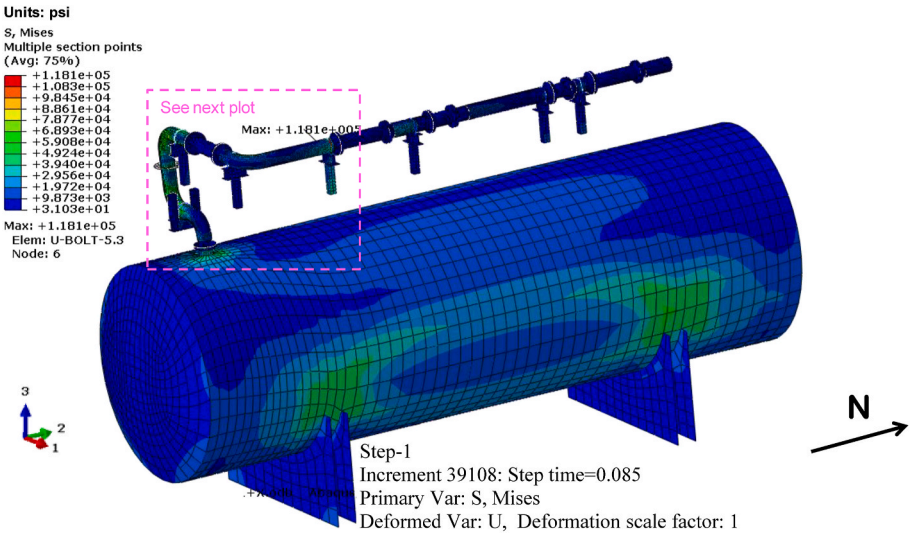

Fig. 36. Effective stress contour at time = 85 ms

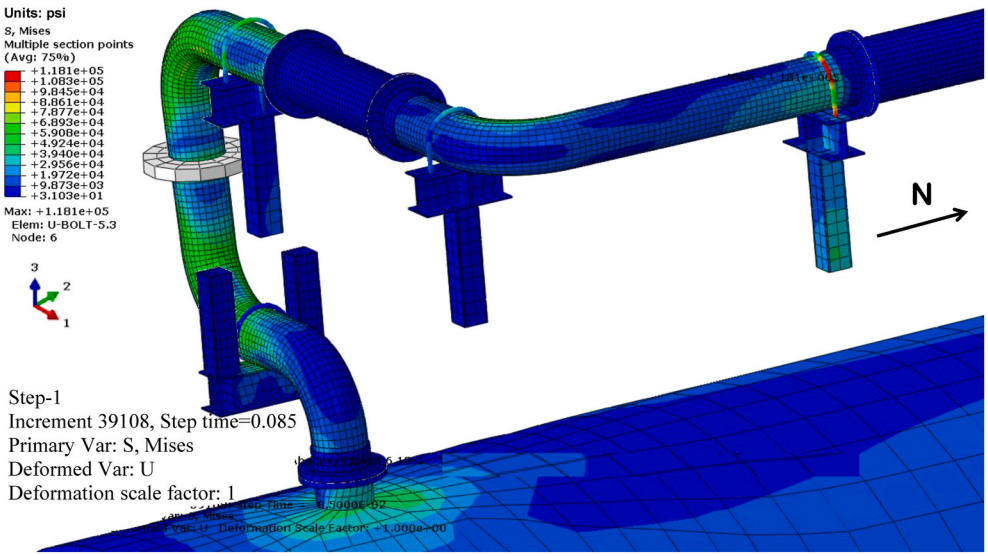

Fig. 37. Maximum von Mises stress 118 ksi appears on the U-bolt at time = 85 ms.

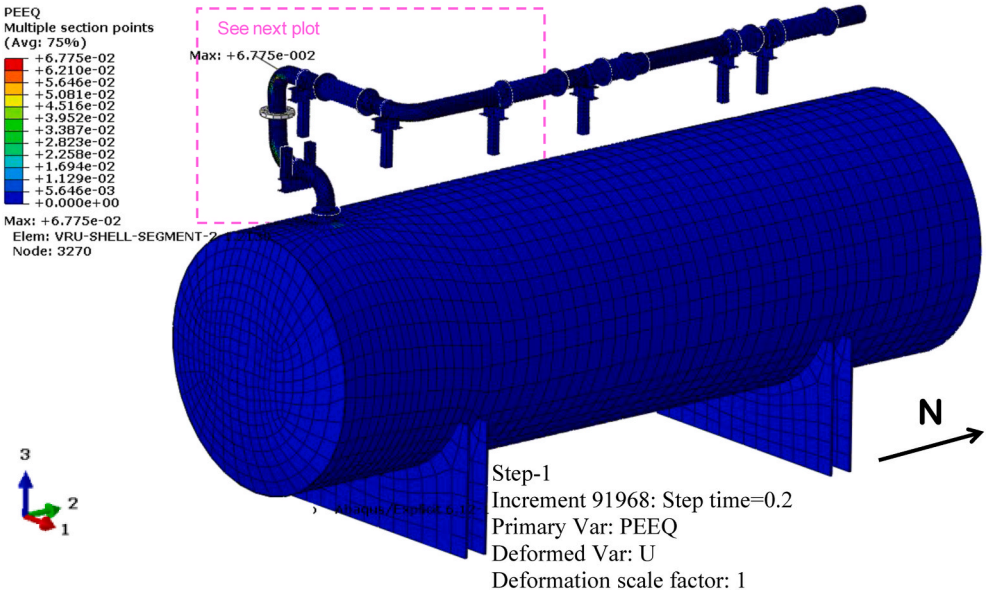

Fig. 38. Plastic strain contour at time = 200 ms

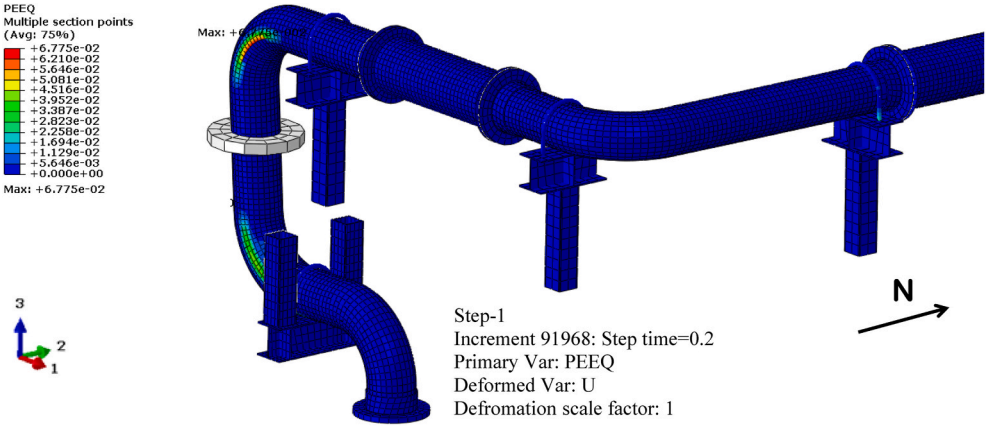

Fig. 39. Plastic strain contour at time = 200 ms (vessel not shown).

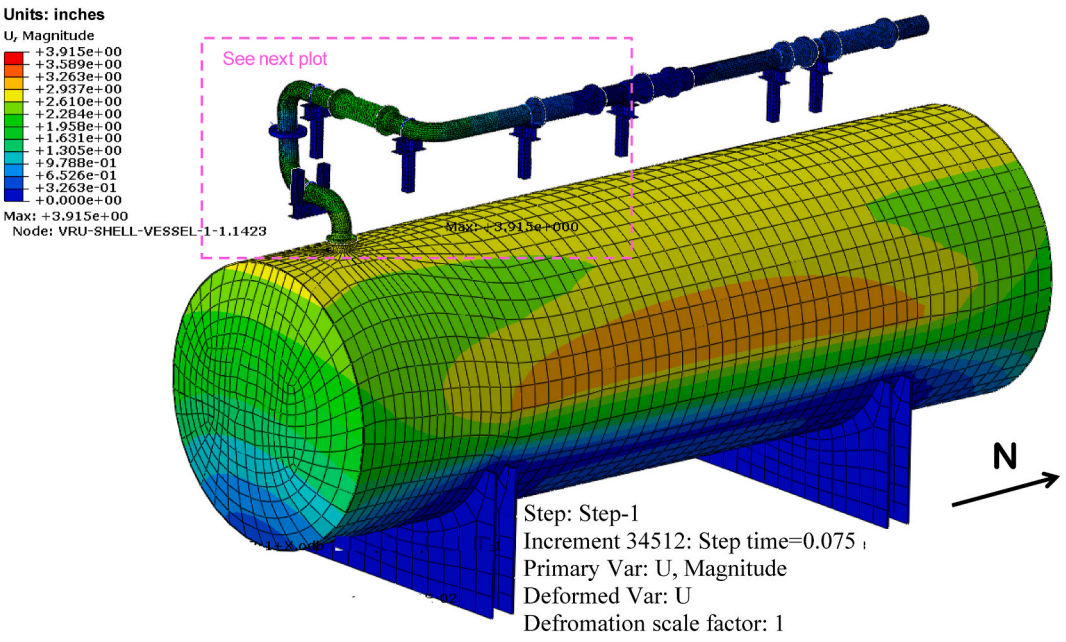

Fig. 40. Deflection contour at time = 75 ms

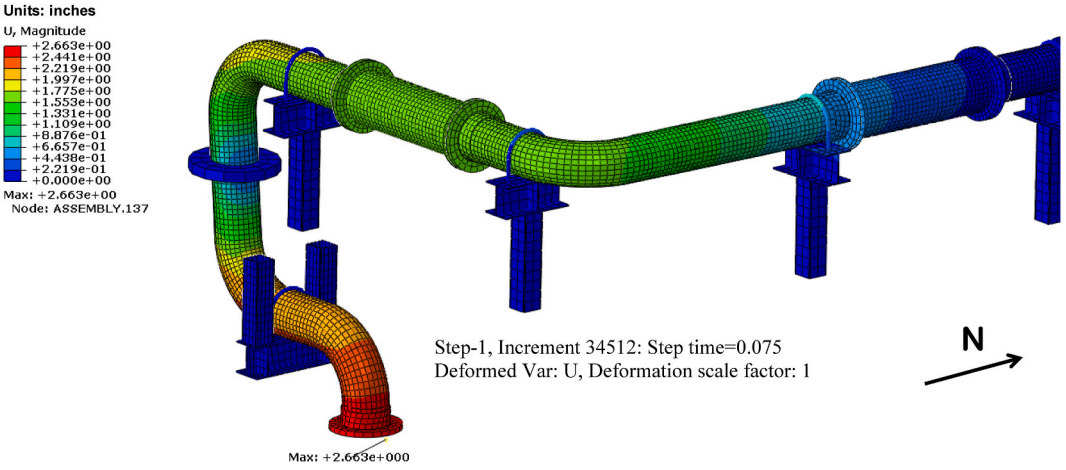

Fig. 41. Deflection contour at time = 75 ms (vessel not shown).

- Materials were assumed to fail if plastic strain reached 5% for connections and 15% for pipes.

3.2. VRU beam model

The FE beam model of the VRU system was constructed of nonlinear beam elements having approximately a one-inch length per element. Pipe supports were also modeled as nonlinear beam elements. Connecting elements (U-bolts) attaching piping segments to pipe supports were achieved through spring connections in both horizontal and vertical directions with upper strength limit. U-bolt stiffness and strength were based on the first principle engineering calculations. Very stiff process segments (e.g., valves) were represented with rigid elements. Other complex piping segments (e.g., flanges) were modeled as beams with modified/simplified section properties. The FE beam model geometries of the VRU system is shown in Fig. 12. Table 1 summarizes pipe materials used. Fig. 13 shows the blast load criteria to be applied to the VRU system. The blast assumed to last 100 ms as shown in Fig. 14. Negative phase was not considered in this study. Fig. 15 indicates the boundary condition assumptions and loading in +Y direction of the FE model.

3.3. Material properties

All elements assumed a nonlinear material model. The material elastic modulus was slightly reduced based on an operational temperature of 300 °F per ASME B31.3 (2002) [14].

The piping material was stainless steel and its behavior was approximated using the stress-strain relationship presented in Fig. 16. Pipe support material was assumed to be mild carbon steel and its behavior was approximated using the stress-strain relationship presented in Fig. 17. Note that Abaqus [5] uses true stress/strain data for material plasticity definition.

3.4. Analysis results for VRU beam model

Figs. 18–26 present the contour plots of von Mises stress, plastic strain, and deflection of VRU system at different times as indicated in plot captions. Fig. 19 indicates high stresses at pipe connections and supports. This is confirmed by Fig. 23 which shows element deletion,

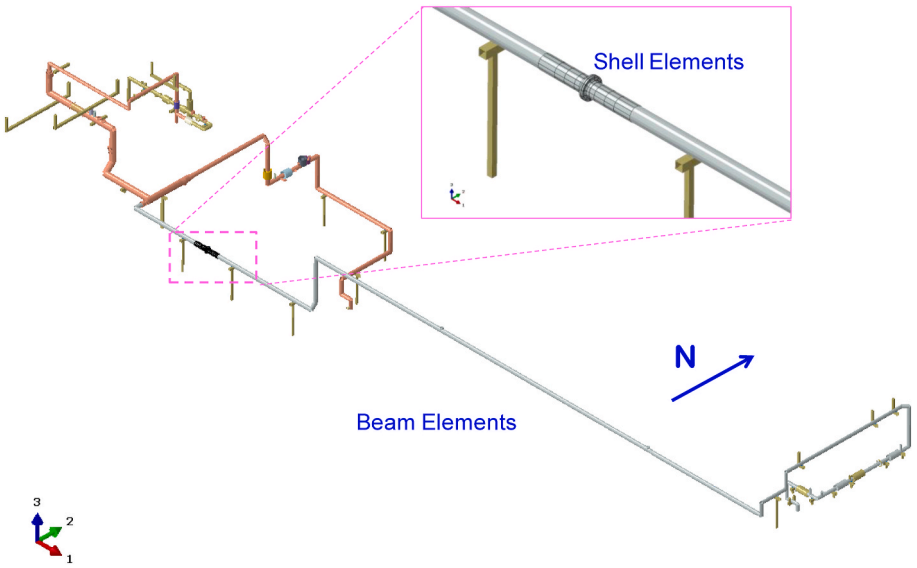

Fig. 42. Global FE beam model with shell element for a pipe flange.

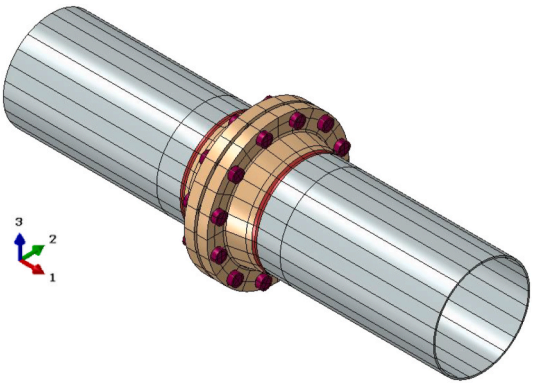

Fig. 43. Flange sub-model (Solid model).

which is indicative of rupture, of one of the pipe connections and supports. Fig. 26 indicates that high deflections are expected as a result of the applied blast loading; a maximum value of 89.6 inches was observed.

3.5. Analysis results considering non-structural masses

Results presented in the previous case did not include the effects of additional masses coming from flanges, valves, and fittings and effects of adjacent piping systems. It was desirable to quantify these effects to a certain degree in the response analyses. In this section, non-structural masses to present flanges, valves, and fittings were calculated and assigned at corresponding locations as shown in Fig. 27.

It was assumed that, at three locations, the VRU system shared the support with other piping systems, as shown in Fig. 28. Similar blast loads were applied to these systems. The blast loading was transferred to supports via U-bolt connections. In other words, these adjacent piping systems did not directly affect the VRU system, rather than put additional blast loads on the supports, effectively reducing their stiffness.

When comparing the stress at blast loading time = 50 ms shown in

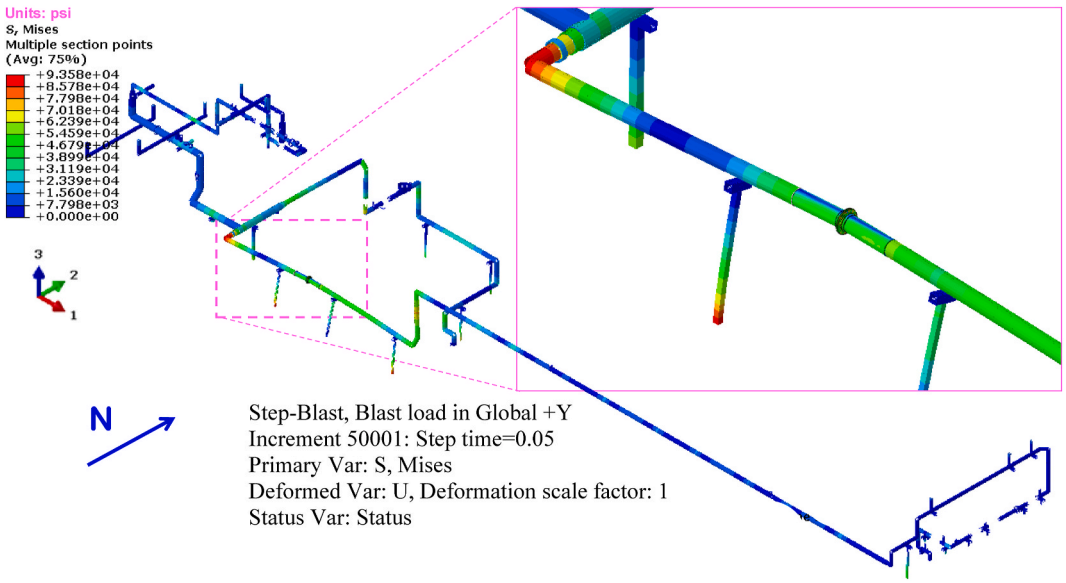

Fig. 44. Effective stress, Blast loads in +Y direction, t = 50 ms

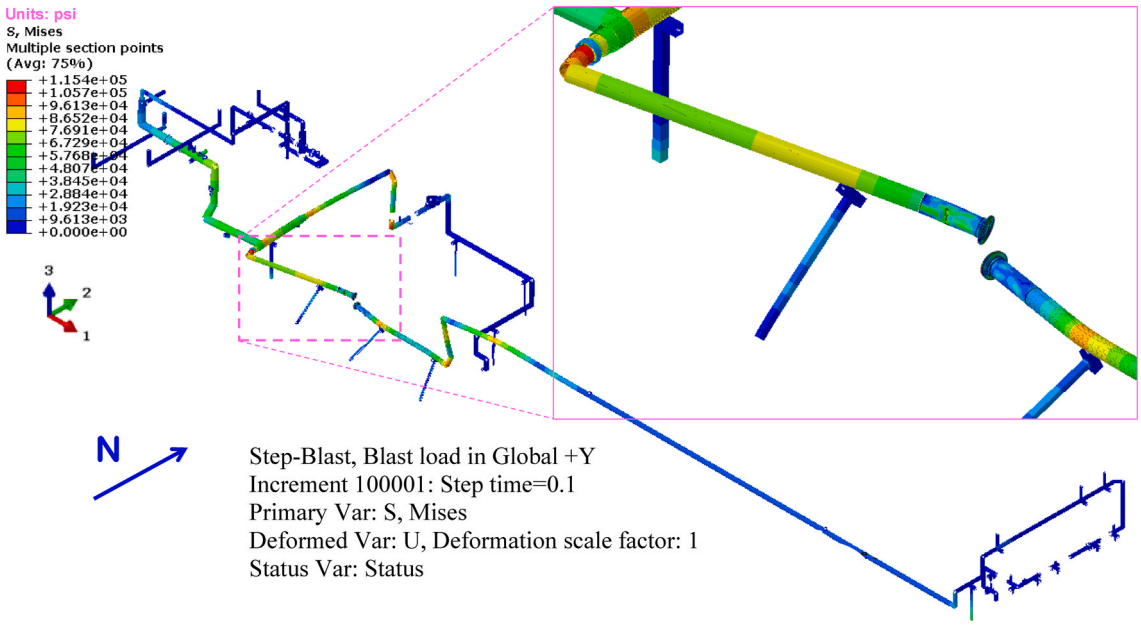

Fig. 45. Effective stress, Blast loads in +Y direction, t = 100 ms

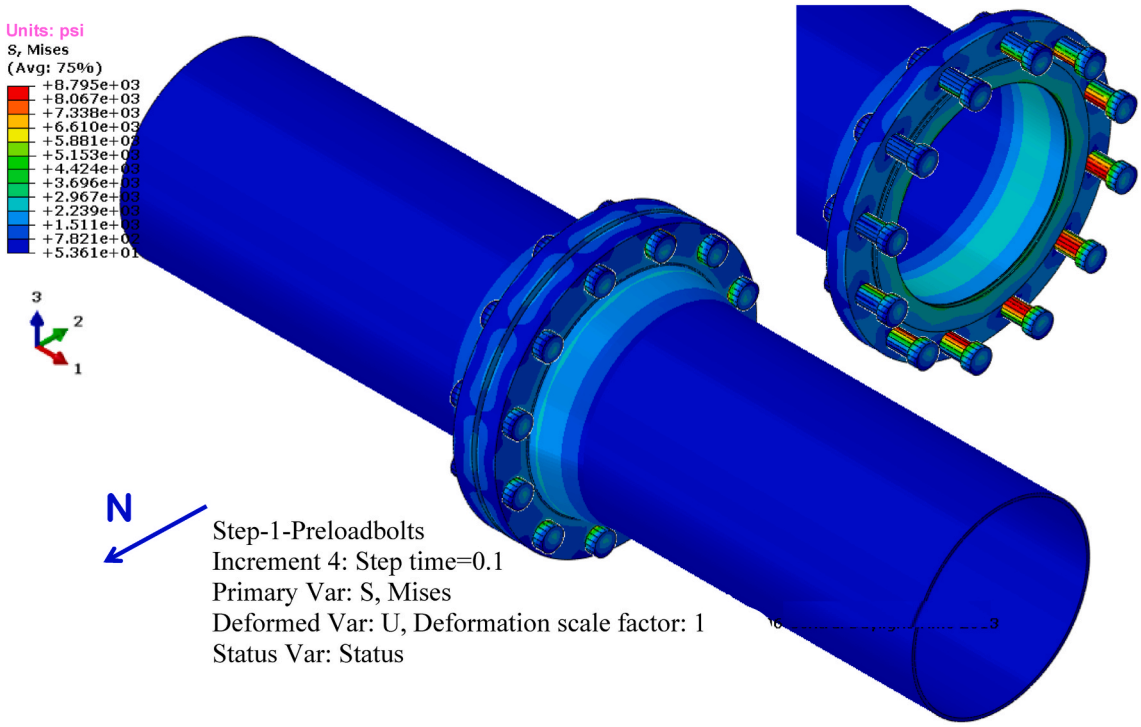

Fig. 46. Effective stress, Bolt load.

Fig. 29 against ones shown in Figs. 18 and 19, the stress at node 67 increased from 43.6 ksi to 50.6 ksi, or 16% increase. The stress, plastic strain, and deflection at the end of blast loading (time = 100 ms) shown in Figs. 30–32 are slightly different than these shown in Figs. 20, Figure 22, and Fig. 25. For example, the maximum deflection increased from 89.6 inches to 101.3 inches with addition of non-structural masses and other piping systems, or 13% increase. Fig. 33 shows the displacement time history at node 67, which shows less 10% increase at time = 100 ms.

3.6. VRU vessel/pipe shell model

Shell model was considered for a pressure vessel and the two pipe lines. Vessel, pipes, instruments and supports were modeled with shell elements. Contact among these components, i.e. between pipes and supports, was modeled explicitly. Flanges were modeled using rigid connections. Connection to a pressure vessel was also modeled. Drag load was applied on pipe surfaces and support surfaces. The FE shell model geometry is given in Fig. 34. Fig. 35 presents the blast loading in the direction perpendicular to the vessel direction which is the principal Y direction with respect to the FE model. Figs. 36–41 show the contour

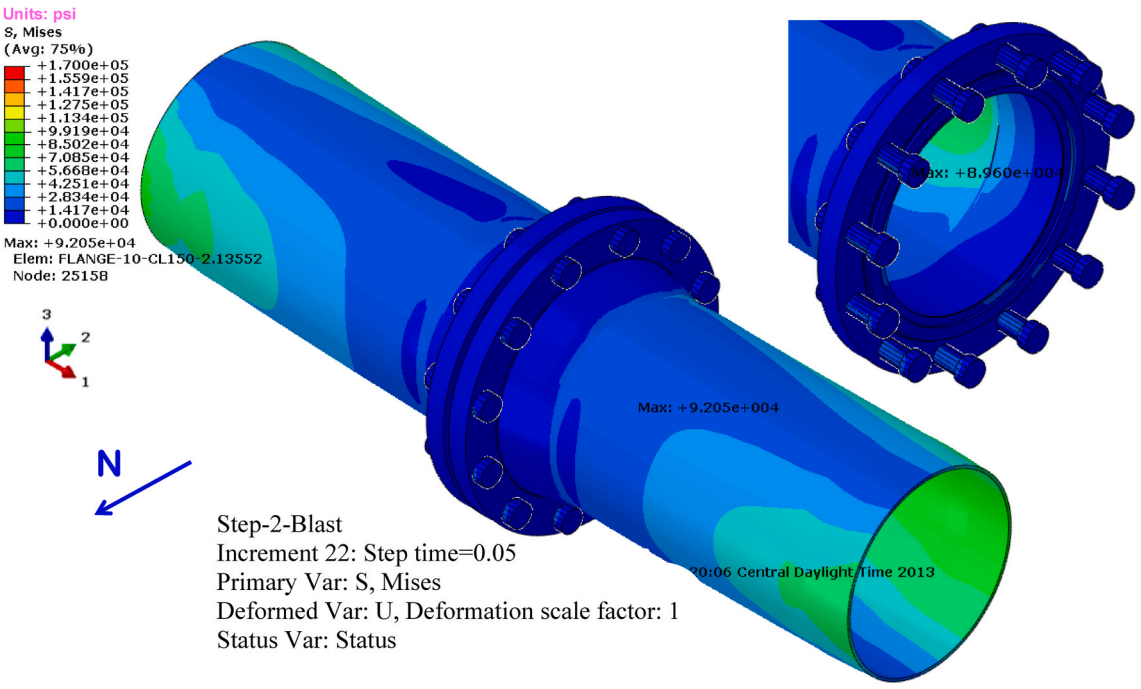

Fig. 47. Effective Stress, Blast loads in +Y direction, t = 50 ms

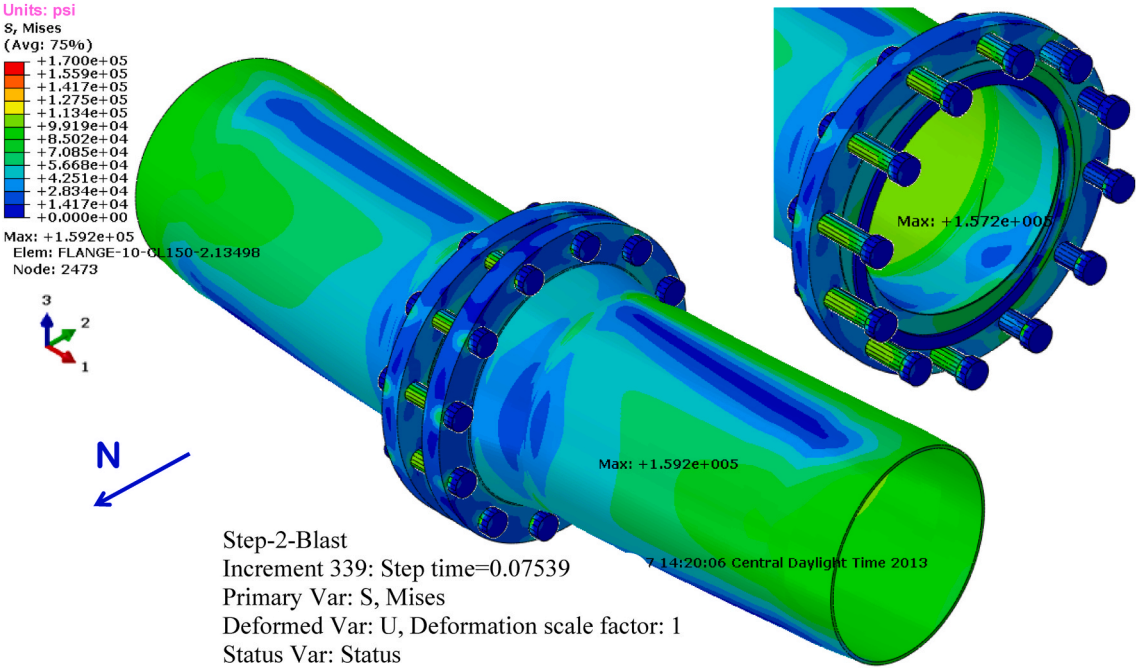

Fig. 48. Effective stress, Blast loads in +Y direction, t = 75 ms

plots of stress, plastic strain, and deflection at the different times during blast loading.

Results show that failure may be dominated by the structural details. For example, Fig. 37 shows that a maximum von Mises stress of 118 ksi appears on one of the U-bolts; or Fig. 39 indicates a maximum plastic strain of 6.77% on pipe elbows. In terms of deflection, a maximum displacement 2.66 inch occurs at the pipe-vessel connection, as shown in Fig. 41. The damage is mostly caused by the movement of the vessel.

3.7. Flange detailed sub-modeling

In a blast event, it is of concern that flanges can open or even fail, and then leakage is an issue. This section examines flange behavior in detail. To this end, in the Beam Model, a flange connection was assumed and modeled explicitly using shell elements. Bolts were modeled as connectors with pretension forces. This global model, shown in Fig. 42, was then fed into a detailed sub-model, shown in Fig. 43, where the flange connection was modeled explicitly using solid elements.

Fig. 44 and Fig. 45 show the contour plots of von Mises stress at t = 50 ms (peak) and t = 100 (end), respectively. Fig. 45 indicates that the

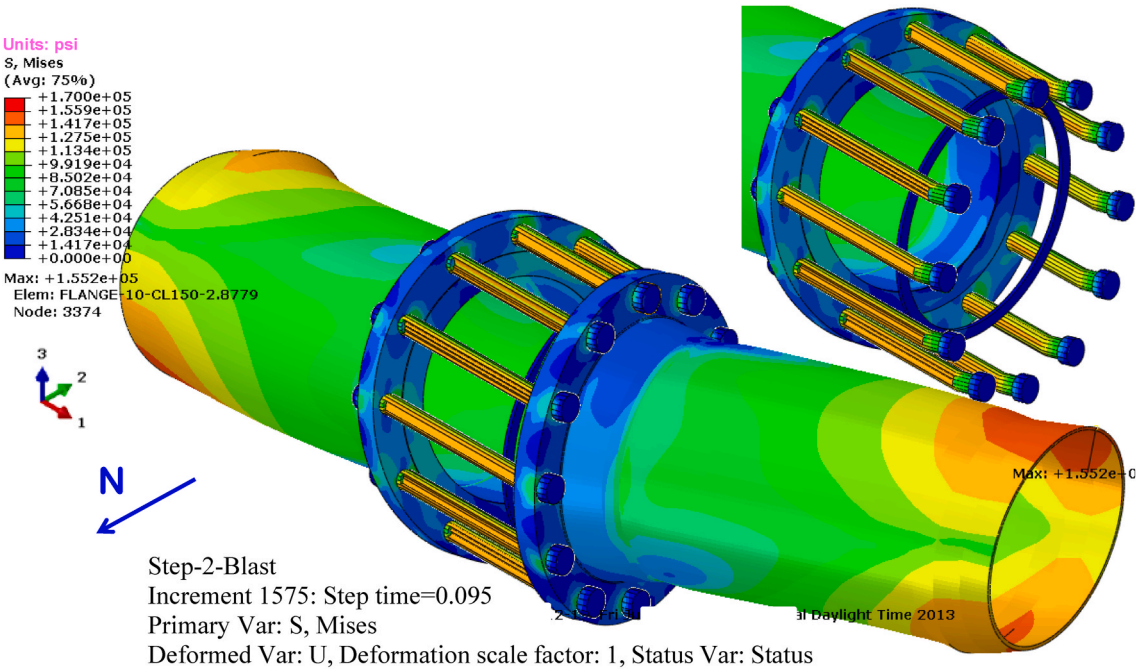

Fig. 49. Effective stress, Blast loads in +Y direction, t = 95 ms

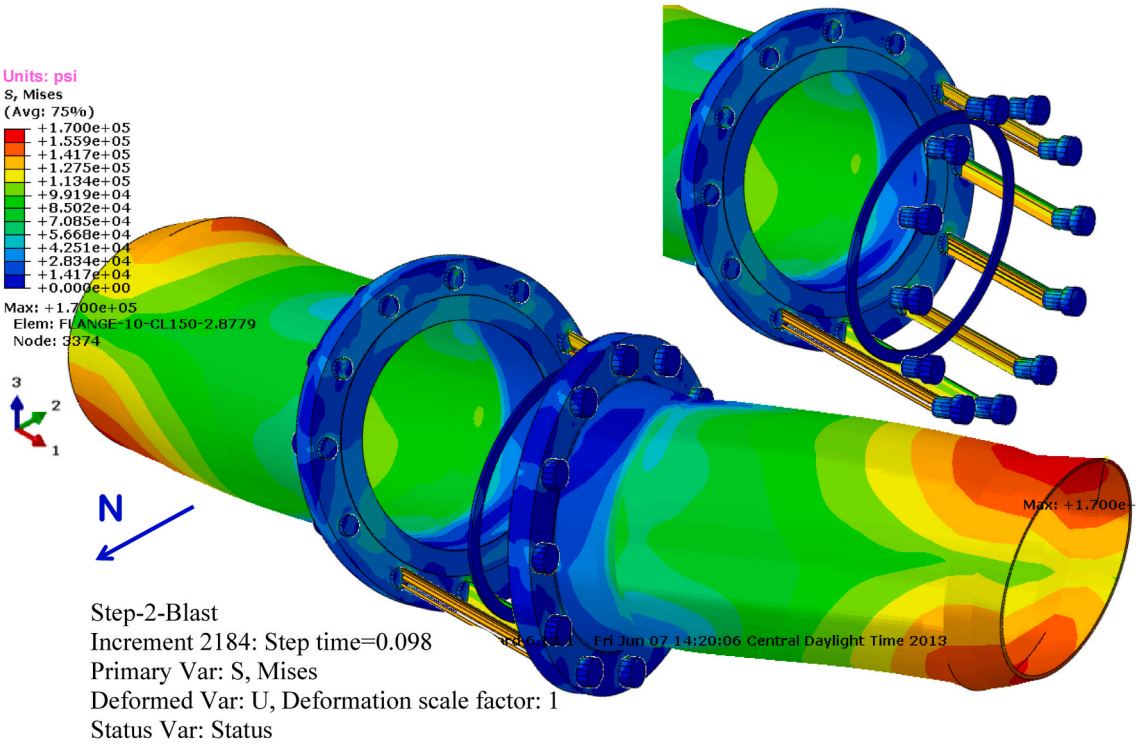

Fig. 50. Effective stress, Blast loads in +Y direction, t = 98 ms

flange connection fails at the end of the blast.

In the sub-model, the bolts are first pre-tensioned to 2585 pounds in one step and then the blast loads are applied to the flange in the sub-sequent step.

Fig. 46 shows the stress contour plot at the end of the bolt load step. Figs. 47–52 show the contour plots of stress and plastic strain at the different times during blast loading.

These plots show that the bolts are highly stressed and eventually fail at the near the end of the blast. This agrees with the flange failure indicated in Fig. 45. In both Global and Sub Models, the flange does not open until t = 50 ms. The Solid Model clearly shows the response of the flange in details. It is recommended that flanges at critical locations (e.g. large bending moment, high differential movements) should be modeled in blast piping analysis.

4. Conclusions

Offshore piping subjected to blast is a complex problem. There are

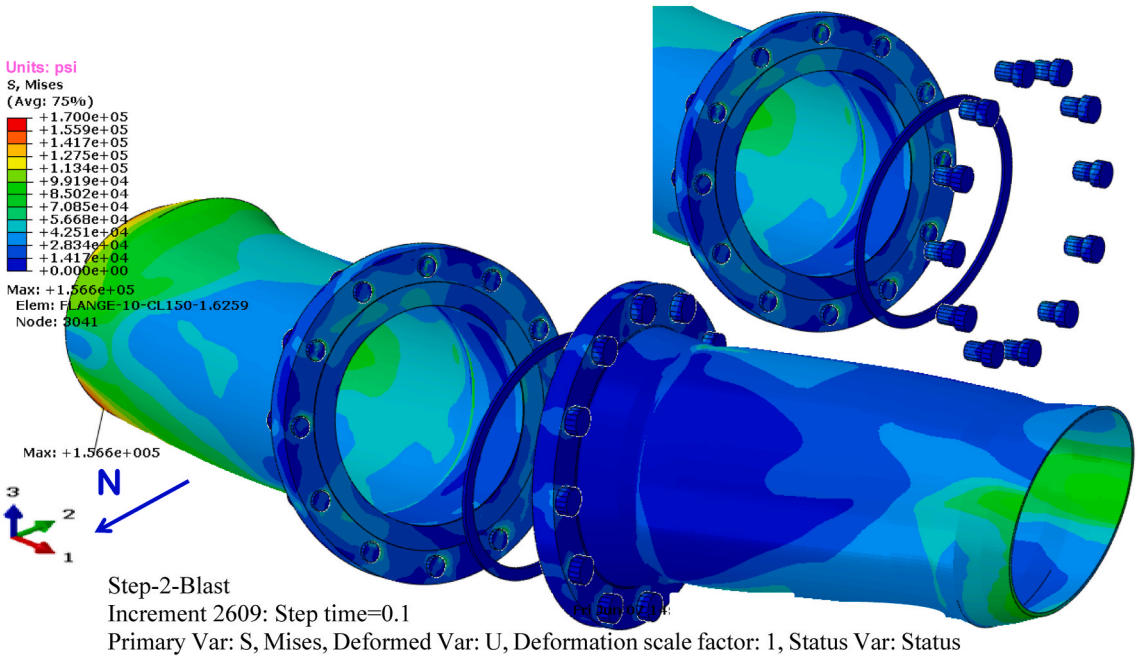

Fig. 51. Effective stress, Blast loads in +Y direction, t = 100 ms

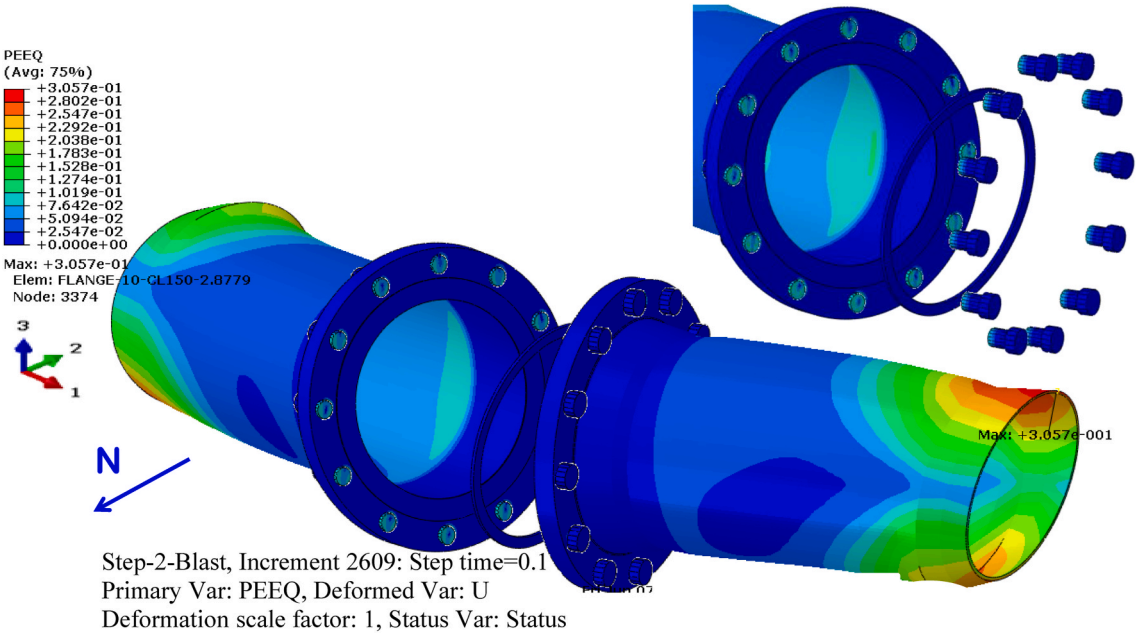

Fig. 52. Plastic strain, Blast loads in +Y direction, t = 100 ms

many aspects that can affect the response of a piping system to blast loading. The ability to perform an advanced numerical analysis such as that described in this paper allows for improved understanding and prediction of response and failure modes of offshore piping systems to explosion threats. Advancements in technology allow detailed numerical studies to become increasingly feasible where physical testing is often not. However, experimental testing should always be performed when possible. The goal of this paper was to discuss the advanced methodology we developed to analyze pipe/vessel systems against blast loadings and how to demonstrate it. By the case studies, the authors have proved that we successfully applied the methodology to a Vapor Recovery Unit piping system modeled at different detail levels. Not all considerations discussed have been included in the case studies. The carried-out advanced FE analyses allowed the following conclusions and observations to be made for case studies presented in this paper.

- Support configuration, flexibility and capacity affect the blast response of the system significantly.
- Non-structural components (masses) and adjacent piping systems affect the overall response of the piping system in consideration. The non-structural masses should be considered in the analysis.
- Response may be affected by the level of modeled details.
- Bolt rupture might control the failure of a piping system. Flange opening/damage should be modeled.
- It is found that the weak points of a pipe system against blast loads are flanges, pipe supports, and connections to equipment.

The advanced analysis methodology for nonlinear piping blast response discussed in this paper can be considered to replace the linear approach used in design practice. Although it requires more time to run analysis compared to simple models, this nonlinear analysis approach not only gives more economic design but also help avoid the weight issue for floating structures.

Author statement

All persons who meet authorship criteria are listed as authors, and all authors certify that they have participated sufficiently in the work to take public responsibility for the content, including participation in the concept, design, analysis, writing, or revision of the manuscript.

Authorship contributions

Ali Sari: Software, Data curation, Conceptualization, Baris Sayin: Investigation, Methodology, Majid Pasbani Khiavi: Validation, Writing – original draft Writing- Reviewing and Editing

Declaration of competing interest

The authors declare that they have no known competing financial interests or personal relationsips that could have appeared to influence the work reported in this paper.

Acknowledgements

This study was funded by Scientific Research Projects Coordination Unit of Istanbul University-Cerrahpasa (Project number: FBA-2018-25947).

References

[1] FABIG/SCI, Protection of Piping Systems Subject to Fires and Explosions, Technical note 8.
[2] 2FB Api, Recommended Practice for the Design of Offshore Facilities against Fire and Blast Loading, 2006.
[3] HSE Report 285, Protection of Piping Systems Subject to Fires and Explosion, Prepared by the Steel Construction Institute, 2005.
[4] S. Yasseri, M. Ocraft, Blast resistant design of process piping: the State of Practice, FABIG Newsletter Issue 55 (May 2010).
[5] Dassault Systèmes Simulia Corp, "Abaqus 6, 12 Analysis User's Manual", 2012.
[6] W.E. Baker, P.A. Cox, P.S. Westine, J.J. Kulesz, R.A. Strehlow, Explosion Hazards and Evaluation, Elsevier Scientific Publishing Company, 1983.
[7] H. Schlichting, Boundary Layer Theory, McGraw-Hill, New York, 1960.
[8] C.E. Needham, "Blast Waves", Shock Wave and High Pressure Phenomena, Springer, 2010.
[9] J.D. Campbell, R.H. Cooper, Yield and flow of low-carbon steel at medium strain rates. Proceedings of the Conference on the Physical Basis of Yield and Fracture, Institute of Physics and Physical Society, London, 1966, pp. 77–87.
[10] P.D. Smith, J.G. Hetherington, Blast and Ballistic Loading of Structures, Butterworth Heineman, 1994.
[11] G.R. Cowper, P.S. Symonds, Strain hardening and strain rate effects in the impact loading of cantilever beams 28, Brown University Division of Applied mathematics Report No, September 1957.
[12] Burgan, B., report"Elevated Temperature and High Strain Rate Properties of Offshore Steels", Offshore Technology Report 2001/020, (SCI).
[13] Eurocode 3: Design of Steel Structures -Part 1-2: General Rules — Structural Fire Design, BS EN 1993-1- 2:2005.
[14] ASME Code for Pressure Piping, B31, ASME B31.3, Process Piping, 2002.